ISSN No:-2456-2165 https://doi.org/10.38124/ijisrt/IJISRT24APR1778

Exploring the Post-Annealing Influence on Stannous Oxide Thin Films via Chemical Bath Deposition Technique: Unveiling Structural, Optical, and Electrical Dynamics

Md. Johurul Islam[1, 2, 4,*], Saidul Islam[2], Mist Toma Khatun[2, 3],
Md. Forhad Hossain[4], Mohammad Jellur Rahman[4] and Suravi Islam[1*]
[1]Industrial Physics Division, BCSIR Dhaka Laboratories, Bangladesh Council of Scientific and Industrial Research (BCSIR), Dhaka 1205, Bangladesh
[2]Dept. of Electrical and Electronic Engineering, Islamic University, Kushtia-7003, Bangladesh
[3]Electronics Division, Atomic Energy Centre Dhaka, Bangladesh Atomic Energy Commission, 4 Kazi Nazrul Islam Avenue, Dhaka-1000, Bangladesh.
[4]Department of Physics, Bangladesh University of Engineering and Technology (BUET), Dhaka-1000, Bangladesh

Abstract: Stannous oxide (SnO_2) thin films have garnered significant attention for their promising applications in various electronic and optoelectronic devices. In this study, we investigate the impact of post-annealing on the structural, optical, and electrical properties of stannous oxide thin films deposited using the chemical bath deposition (CBD) technique. The thin films were prepared on a Borosilicate glass substrate, followed by a controlled annealing process to enhance their performance. Structural analysis was conducted using techniques such as X-ray diffraction (XRD) to examine the cubic crystalline structure and the crystallite size increase induced by post-annealing. The results revealed alterations in grain size from the SEM and the purity of samples confirmed from EDX results. The optical properties of the Stannous oxide thin films were examined using UV-Vis spectroscopy. The optical absorption and bandgap characteristics were analyzed to understand how post-annealing influences the optical behavior of the thin films. Where the optical absorption was 320nm and the bandgap ranges were 3.86eV to 3.83eV. Furthermore, the electrical properties of the thin films were evaluated semiconducting nature, and conductivity increased with rising post-annealing. The findings from this study contribute to the understanding of the role of post-annealing in tailoring the properties of Stannous oxide thin films. The optimization of structural, optical, and electrical characteristics is crucial for their successful integration into electronic and optoelectronic devices.

Keywords:- *Sno_2 Thin Films; CBD; X-Ray Diffraction (XRD), UV-Vis Spectroscopy, Post-Annealing.*

I. INTRODUCTION

In recent years, transparent conducting oxides have been great research focal points [1–4]. SnO_2 is an interesting semiconductor material and can function as both P-type and N-type semiconductor due to its non-stoichiometric nature having a wide bandgap 3.6-3.9 eV [5, 6].

SnO_2 thin films have a wide range of applications including as transparent active layers in SnO_2 silicon solar cells [7] and transparent electrodes in display devices as liquid crystal displays (LCDs), photochemical devices, optoelectronic devices, light detectors, transparent conducting electrodes, heat-reflective mirror, far-infrared detectors, gas sensors, biosensors, electrically conductive glass, antireflection coatings and thin film resistors [8-12]. Generally, SnO_2 is a compound that can exist in different phases, namely tetragonal, cubic, or orthorhombic phases. The optical characteristics of SnO_2 can vary considerably reliant on the structural phase. The phase of SnO_2 can be changed by modifying the deposition method and time, also annealing temperature. There are several techniques available to prepare SnO_2 thin films, including Spray pyrolysis, plasma polymerization, screen printing, spring coating, RF sputtering, physical vapor deposition, pulsed laser evaporation, metal-organic chemical vapor deposition (MOCVD), and chemical bath deposition (CBD) method [13]. Among them, the CBD method is widely used due to its simplicity, affordability, and ability to deposit large areas of thin films with slight chemical convention. This method uses a stable chemical reaction to deposit a thin film. Furthermore, the CBD method can produce thin films with various structures such as nanocrystal, microcrystal depends on different conditions [14].

ISSN No:-2456-2165 https://doi.org/10.38124/ijisrt/IJISRT24APR1778

The main aim of this research is to describe how the structural, morphological, optical, and electrical properties of SnO_2 thin films are affected by post-annealing. These samples were fabricated on Borosilicate glass substrates using the CBD method.

II. EXPERIMENTAL

The thin films of SnO_2 were synthesized by exhausting Stannous chloride dihydrate [$SnCl_2.2H_2O$], Sodium Hydroxide [NaOH] and Urea [$CO(NH_2)_2$]. The chemical used to synthesize thin films was sourced from Merck Germany. All primary ingredients, including ethanol and deionized water (DI) water, were maintained at analytical reagent grade, also utilize without refinement. The glass substrates were purified prior to the deposition of thin films to prevent any impact on the films' properties. Microscope slides measuring 76 × 26 × 1 mm^3 were chosen for the substrates. First, the slides were washed using cleansing agent and DI water and were then immersed in H_2SO_4 for approximately one hour. After the cleaning process, the substrates were rinsed with DI water and dried in air oven at 80°C temperature. These purified glass slides were later applied for depositing thin films.

To deposit SnO_2 thin film via CBD method, 200ml 0.5M $SnCl_2.2H_2O$ was collected in washed glass tube. 15ml 1M $CO(NH_2)_2$ was mixed with the Stannous chloride dihydrate solution. Subsequently, the solution was stirred for half of hours. After that, 1M sodium hydroxide was mixed gradually to form a complex solvent until the solution reaches a pH of 11. The solution was stirred at 25°C temperature for half an hour. The next step was sonication of the suspension in an Ultrasonic bath for 10 minutes. Then, a clean glass substrate was submerged in the solution and left at room temperature for 48 hours. A further, the immersion period, a thin film of SnO_2 was synthesized on the Borosilicate glass slid. The deposited sample was rinsed with DI water and dried using a vacuum oven at 50°C temperature for one hour. Finally, the synthesized thin films were sintered at 500°C and 600°C in the furnace for 2 hours. Fig. 1 displays the various steps involved in the deposition of the SnO_2 thin films using CBD method.

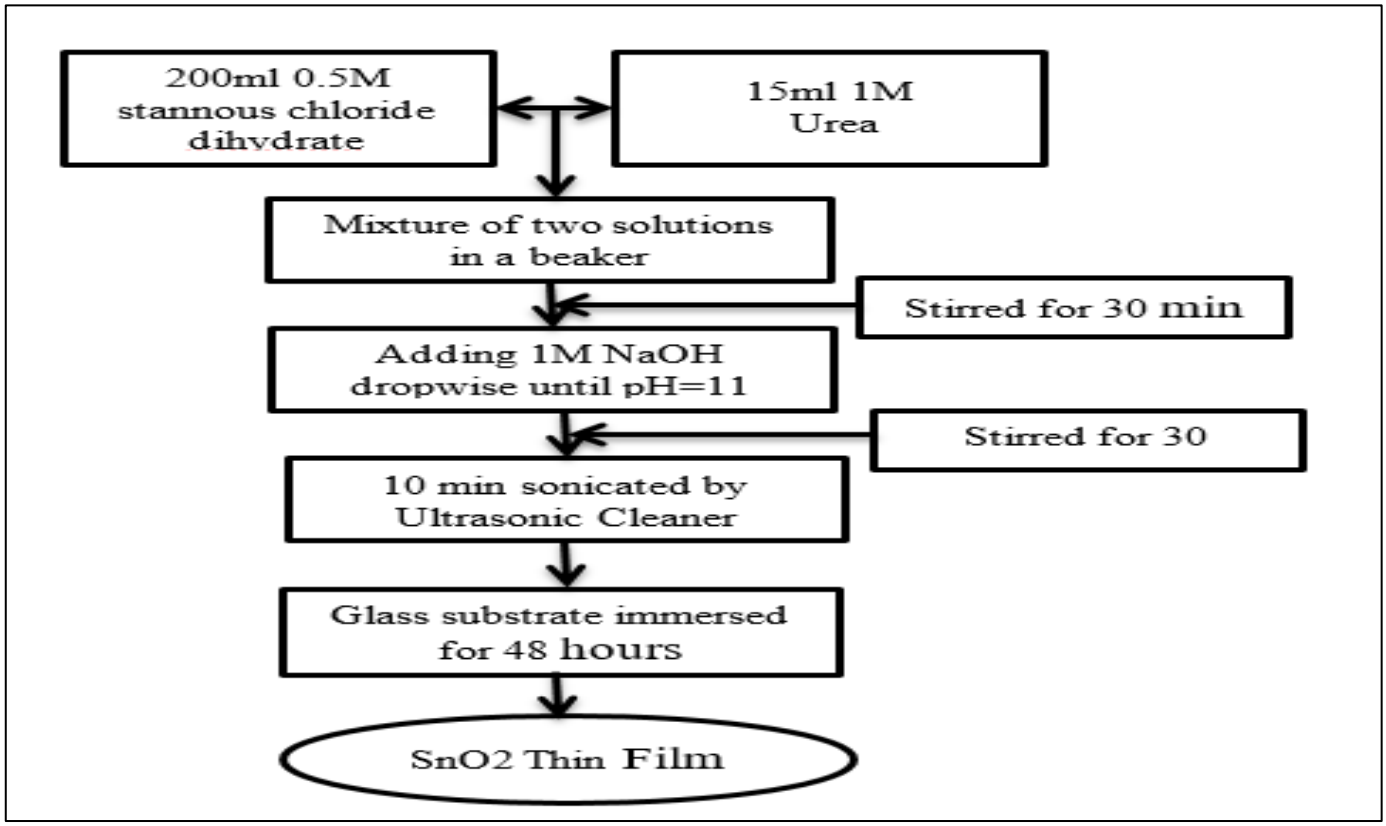

Fig 1: Deposition Steps of the SnO_2 Thin Film

The SnO_2 thin films were analyzed for their structural properties using a X-ray Diffractometer (Bruker D8 Advance, Bruker, Germany) with CuKα radiation of wavelength λ=1.5406 Aº. X-ray diffraction (XRD) patterns were recorded peak intensities to their 2Θ degree values from 20º to 80º with scanning speed of 0.02 degree/sec. The research focused on studying the surface morphology and chemical composition of SnO_2 thin films which was done by using a Scanning Electron Microscope (SEM) (Model JSM-6490LA, Jeol, Japan) in secondary electron emission mode. The optical absorption features of the films were analyzed through comparing them with a plain glass substrate using a UV-1601, UV-Vis spectrophotometer made by Shimadzu, Japan in the range of 200 nm to 1100 nm. Additionally, the conductance of the samples was calculated by using an Electrometer analysis system (6517B, Keithley, USA).

ISSN No:-2456-2165 https://doi.org/10.38124/ijisrt/IJISRT24APR1778

III. RESULTS AND DISCUSSION

A. Structural Properties:

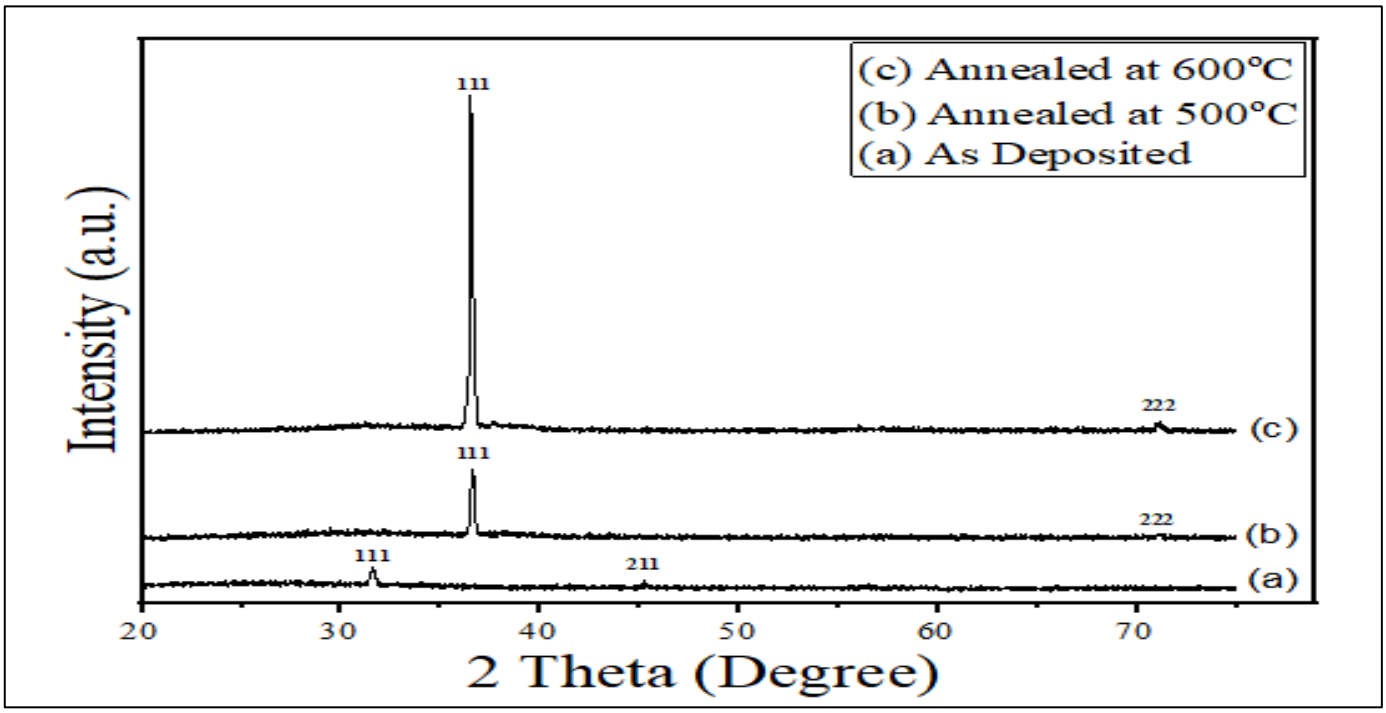

Fig 2: XRD Patterns of SnO_2 thin Films at Different Annealing Temperature

Fig. 2 shows XRD patterns of SnO_2 thin films deposited CBD technique and annealed the synthesized samples at 500℃ and 600℃. This analysis reveals that SnO_2 thin film deposited by the CBD process, exhibits a fine polycrystalline cubic structure and the phase is remain same after annealed at 500℃ and 600℃. All the SnO_2 polycrystalline films appear peaks that correspond mostly to the SnO_2 (111), (211) and (222) crystalline planes. The strongest peak of the deposited thin film is at 2θ=31.67° from diffraction pattern which detected reflections planes (*hkl*) conforming to the peak being 111 and when the deposited thin film annealed at 500℃ and 600℃ there is a blueshift occurs. After annealing at 500℃ and 600℃ the strongest peak position corresponding to (111) plan is 2θ=36.7° and 36.58° respectively. For the deposited thin film, the other peak is found at 2θ=45.38° which observed reflections planes (*hkl*) corresponding to the peak is (211). An alteration in the ideal alignment is observed from (211) to (222) after annealing the deposited thin film at 500℃ and 600℃. Again, annealing at 500℃ and 600℃ the weak peak position corresponding to (222) plan is 2θ=71.26° and 71.18° respectively. The diagram shows that SnO_2 particles are either semicrystalline in nature or they have a very small crystalline size, as indicated by the weak peaks [15]. These findings are consistent with the JCPDS card No.01-071-5329. [16]. As the annealing temperature increases, the peaks in XRD turn sharper, the particle size grows larger, and the crystallinity improves. These results are in alignment with other studies [17].

X-ray diffraction is a convenient technique for calculating the crystallite size of nano crystalline materials. To determine the crystallite size (D), the Debye-Scherrer equation is applied [18].

$$D = K\lambda / \beta cos\theta \quad \text{---------- (1)}$$

In this equation, K is a constant related to crystallite shape and is typically taken as 0.9. λ is the wavelength of X-ray, which is 1.5406 Å. β represents the full width at half maximum (FWHM) intensity of the peak in radians, and θ is the Bragg's diffraction angle. Average D illustrate in **Table 1**. The formula to calculate the strain (ε) of SnO_2 samples at diverse annealing temperatures is:

$$\varepsilon = \beta cos\theta / 4 \quad \text{---------- (2)}$$

Here, β represents the full width at half-maximum of the preferential peak in radian. The dislocation density (δ) is defined as the length of dislocation line per unit volume. In the case of SnO_2 samples, the dislocation density (δ) can be calculated with subsequent formula:

$$\delta = n/D^2 \quad \text{---------- (3)}$$

Where, n is a constant equal to 1, and D represents the crystallite size. The minimum dislocation density is achieved when n is equal to 1.

ISSN No:-2456-2165 https://doi.org/10.38124/ijisrt/IJISRT24APR1778

Table 1: Demonstrates Structural Parameters of SnO2 Samples at Different Annealing Temperatures

Sample Name	Peak Position 2θ°	Reflections Plane (hkl)	Calculated Spacing d (Å)	Standard Spacing d (Å)	Crystallite size (nm)	Average Crystallite size D (nm)	Dislocation Density (δ) * 10^{-3}	Strain (ε) *10^{-3}
As Deposited	31.67	111	2.82226	2.82678	22.37362	25.4656	0.00199	0.00154
	45.38	211	1.99564	1.99610	28.55768		0.00122	0.00121
Annealed at 500℃	36.7	111	2.82226	2.82288	33.29311	27.5695	0.00068	0.00090
	71.26	222	1.41113	1.41095	30.79695		0.00347	0.00204
Annealed at 600℃	36.58	111	2.82226	2.82426	38.17927		0.00090	0.00104
	71.18	222	1.41113	1.41050	16.95973	32.0450	0.00105	0.00112

B. Morphological Properties: SEM Analysis

Crystal substrate-assisted CBD technique was used to deposit SnO2 films. The films' surface morphology is shown in Fig. 3(a-c). The images were taken at different annealing temperatures - (a) As Deposited, (b) Annealed at 500℃, and (c) Annealed at 600℃. As per these images, it is evident that the structure and morphology of SnO_2 thin films vary per annealing temperature. The particle sizes increase as the annealing temperature rises, whereas they decrease corresponding to the energy band gap [19]. Using the SEM images, the particle sizes of the entire thin films sample at various annealing temperatures were dignified exhausting the ImageJ software. The average particle sizes for those samples were estimated to be approximately 60 nm, 85 nm, and 110 nm, respectively.

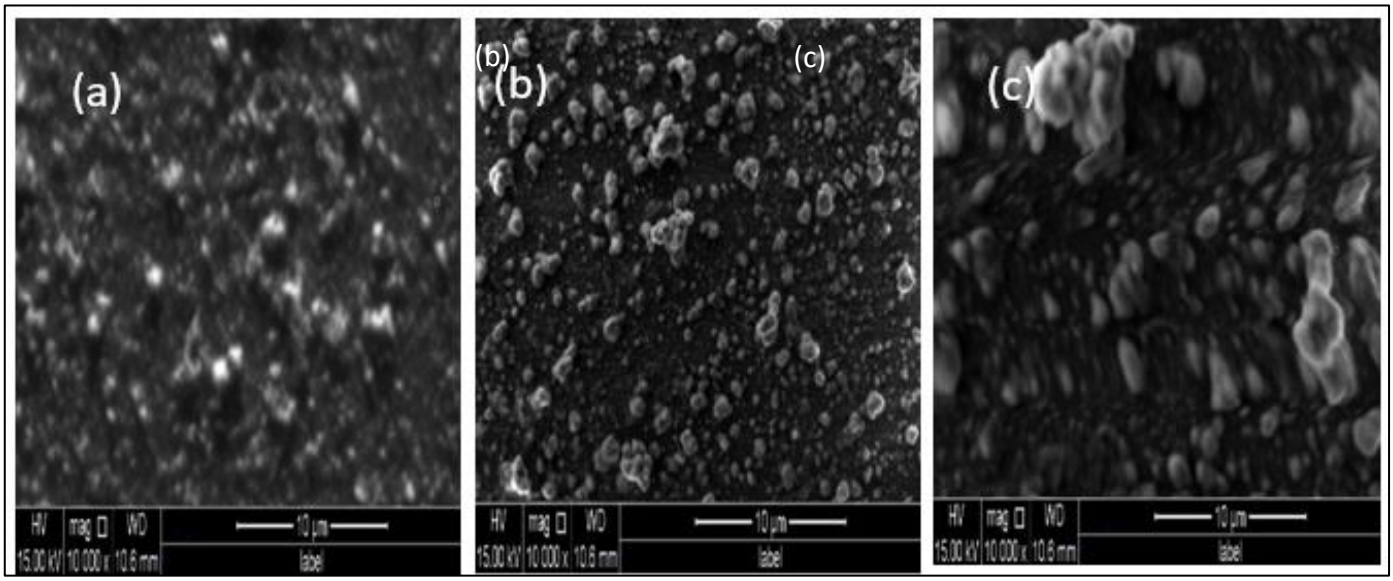

Fig 3: SEM Micrographs of SnO_2 thin Films at (a) As Deposited, (b) Annealed at 500℃ and (c) Annealed at 600℃.

C. Element Analysis: EDX

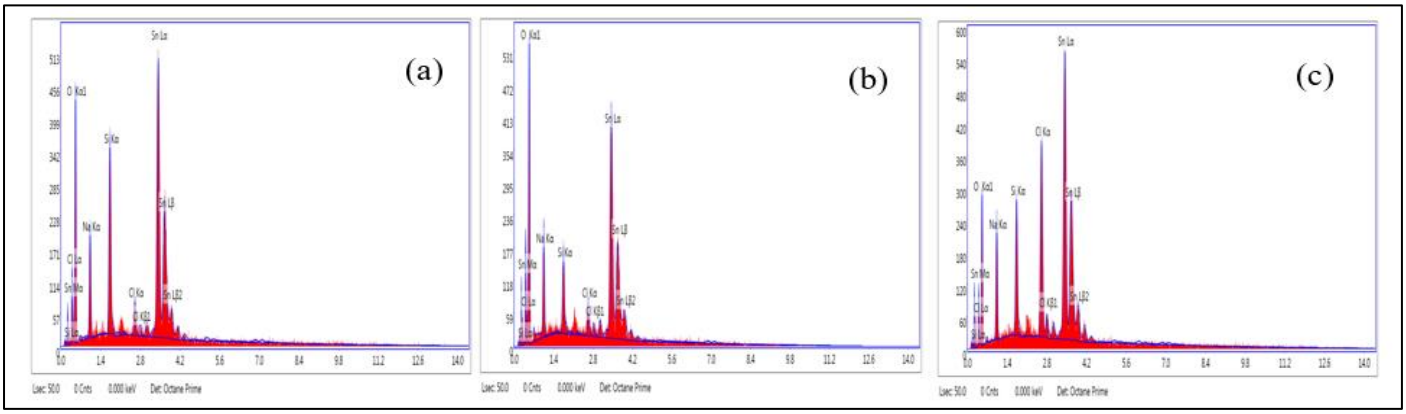

Fig 4: EDX Spectra of SnO_2 Thin Films at (a) As Deposited, (b) Annealed at 500℃ and (c) Annealed at 600℃.

ISSN No:-2456-2165 https://doi.org/10.38124/ijisrt/IJISRT24APR1778

Energy-dispersive X-ray spectroscopy (EDX) is a method utilized to analyze the elemental percentage in a film and characterize its chemical properties. **Fig. 4**(a-c) displays the EDX spectra and element scattering of SnO_2 thin films at various annealing temperatures. The first image (a) shows the film as deposited, the second (b) shows it after annealing at 500°C, and the third (c) shows it after annealing at 600°C.

Fig. 4 confirms the presence of Sn, O_2, Na, Cl and Si in all the SnO_2 thin films at different annealing temperature. From The EDX microanalysis indicates the presence of tin (Sn) and oxygen (O_2). Besides these two elements, there are also a few other elements present in small quantities. These elements may have resulted from the other components in the solution and the Si-based glass substrate. The measurement of EDX microanalysis confirms that the films are, in fact, SnO_2 thin films.

D. Optical Properties

The absorption spectra of SnO_2 thin films on glass slid at various annealing temperatures are shown in Fig. 5 (a-c), using UV-visible spectroscopy. The optical absorption of thin films was analyzed in the wavelength range 200-1100 nm. The absorption spectra of SnO_2 thin films at different annealing temperatures showed absorption (300-350nm) because of SnO_2 crystallite development, possibly cause by tin dioxide crystals formation [20]. From **Fig. 5** it is shown that the optical absorption of the thin films is minimum in the ultraviolet region and increasing in the 250-300 nm range. From fig.5 it is observed that the absorption of the SnO_2 also increases corresponding to the annealing temperature. According to the relation between the absorbance and transmittance it has been observed that the transmittance of the SnO2 thin film decreases as the annealing temperature increases.

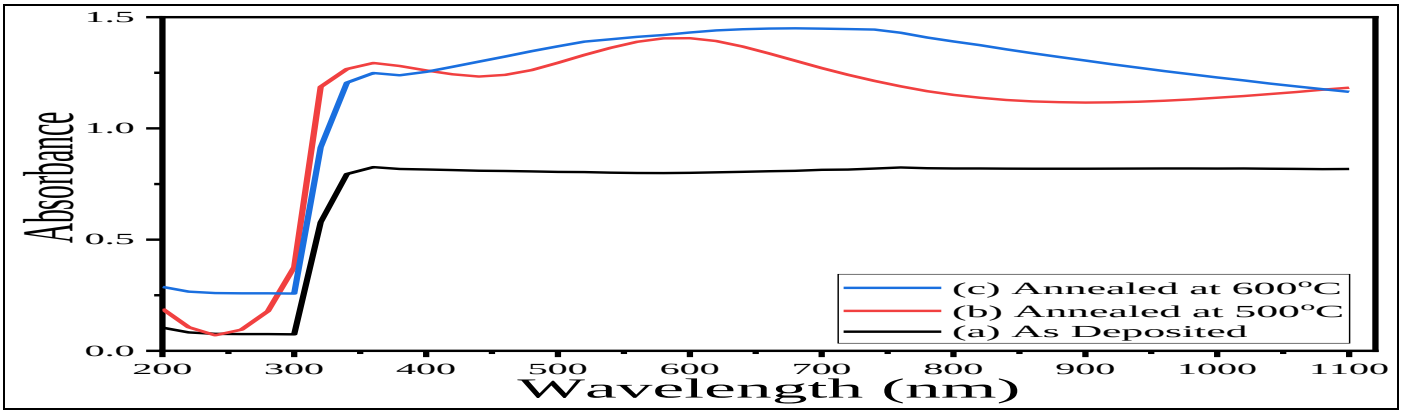

Fig 5: The UV–vis Absorbance Spectra of SnO2 thin Films at Different Annealing Temperature.

➢ *Band Gap Calculation for SnO_2 Thin Films*

The optical band gap can be determined by using various techniques among them; tauc plot technique has significance. The SnO_2 thin film band gap is also calculated by using this method. Tauc developed and validated a technique for determining the band gap of amorphous germanium by studying its optical and electronic properties. In this approach, optical absorbance data is plotted against energy in a suitable manner [21]. Davis and Mott developed the method further for amorphous semiconductors and showed that the difference between photon energy and band gap impacts optical absorption strength [22, 23], as demonstrated in the equation below:

$$(\alpha h\nu)^{1/n} = A(h\nu - Eg) \quad \text{---------- (4)}$$

Here, h represents Planck's constant, ν represents the frequency of the photon, α represents the absorption coefficient, Eg represents the band gap, and A is a proportionality constant. The exponent value indicates the type of electronic transition, whether they are allowed or forbidden, and whether it is direct or indirect.

The basic optical absorption processes are usually dominated by the allowed transitions which result in either n=1/2 or n=2 for direct and indirect transitions respectively. Therefore, the fundamental process for a Tauc calculation is to collect optical absorbance data for the sample being studied, which covers an array of energies from below the band gap transition to above it. To identify the correct transition type the $(\alpha h\nu)^{1/n}$ versus $(h\nu)$ should be plotted and tested with $n=1/2$ or $n=2$ to determine which provides a better fit [24].

The energy gap within a semiconductor leads to an important character to determine the optical absorption edge. The graph in Fig. 6 shows the relationship between $(\alpha h\nu)^2$ and Energy (eV) for the direct transition of SnO_2 thin films at various annealing temperatures. By extrapolating the straight-line section of the $(\alpha h\nu)^2$ vs Energy (eV) curve and finding the intercept on the energy axis, the direct band gap energy can be obtained [25]. The optical direct band gap of SnO_2 thin films was measured at different annealing temperatures, namely (a) As Deposited, (b) Annealed at 500°C, and (c) Annealed at 600°C. The recorded values for the band gap were 3.86 eV, 3.84 eV, and 3.83 eV, correspondingly. These values are consistent with the testified values (ranging from 3.6 eV to 3.9 eV) [26]. From the observations presented in Fig. 6, it can be inferred that the band gap of SnO2 thin films reduces as the annealing temperature increases, and also decreases as the crystallite size of the films increases [27].

ISSN No:-2456-2165 https://doi.org/10.38124/ijisrt/IJISRT24APR1778

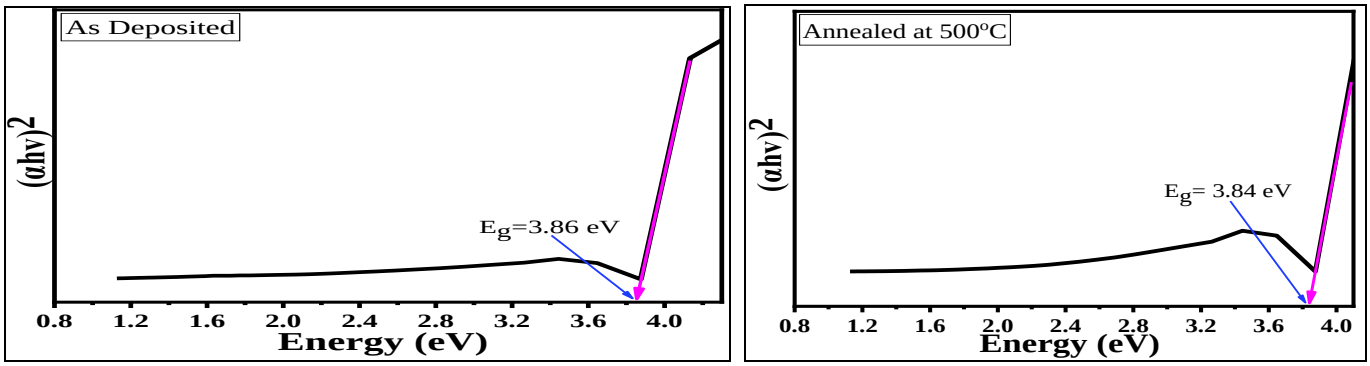

(a) As Deposited. (b) Annealed at 500°C.

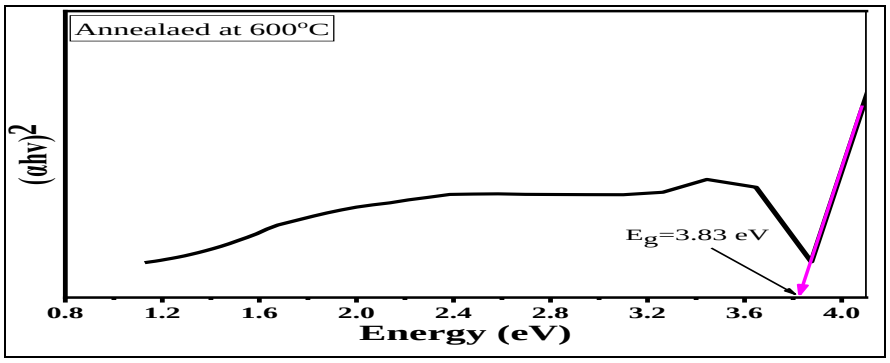

(c) Annealed at 600°C.

Fig 6: Tauc Plot from UV-Vis Analysis for SnO2 thin films at Different Annealing Temperature

E. DC Conductivity Measurement

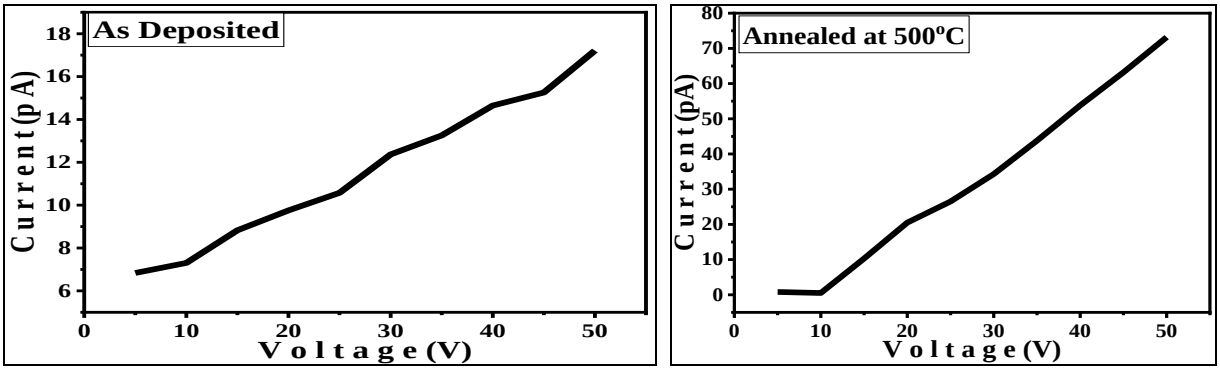

(a) As Deposited. (b) Annealed at 500°C.

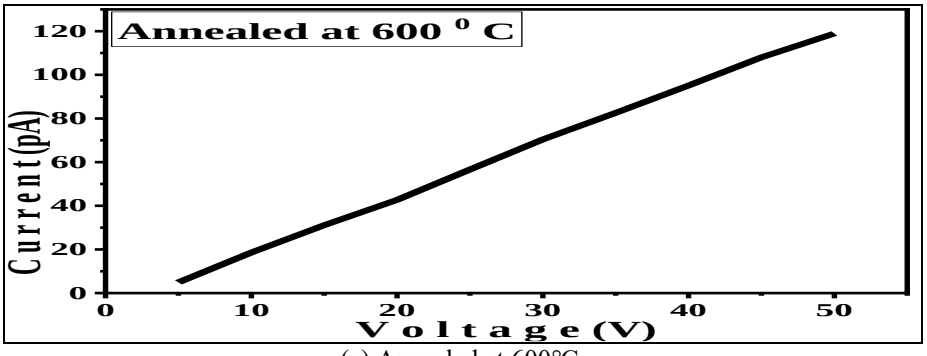

(c) Annealed at 600°C.

Fig 7: Current (pA) vs Voltage (V) Curve of SnO_2 thin Films at different Annealing Temperature

Fig. 7 depicts the Current (pA) vs Voltage (V) curves of SnO_2 thin films at various annealing temperatures. As evident from the graph, the current is amplified respect to voltage increasing. At 50DV applying for each sample the values were approximately 17.25 pA, 73.63 pA, and 120 pA respectively for SnO_2 thin films where (a) As Deposited, (b)

ISSN No:-2456-2165 https://doi.org/10.38124/ijisrt/IJISRT24APR1778

Annealed at 500℃ and (c) Annealed at 600℃. The results establish that the conductivity improves with corresponding to the annealing temperature and decreasing related with the optical band gap [28]. From the optical analysis it is seen that the band gap also decreasing with increasing the conductivity and annealing temperature also. From this analysis it is clear that the relation between conductivity and band gap is reverse.

IV. CONCLUSIONS

In summary, SnO_2 thin film was fruitfully synthesized on borosilicate glass slide via CBD methods and the post-annealing effect on various properties was also studied. . The XRD patterns of SnO_2 thin films at different annealing temperature deposited by CBD methods are shown crystalline cubic phase and the crystallite size increasing respect to annealing temperature. SEM micrographs revels the surface morphology of the thin films. EDX observation confirmed the presence of Sn and O_2 in the samples. From the UV-visible spectroscopy, the sample's absorbance was found at ultraviolet and it increases with increasing the annealing temperature. The direct band gap varies with different annealing temperature. The optical direct band gap of SnO_2 thin films deposited is 3.86eV, annealed at 500℃ is 3.84eV, and annealed at 600℃ is 3.83eV respectively. The band gap of the SnO_2 thin film is decreasing with temperature condition and decreasing with increasing the crystallite size of the films. Based on the I-V curve, we also found that the current escalations corresponding to the voltage which confirms that the SnO_2 thin films exhibit semiconducting properties. Additionally, as per the principles of semiconductor properties, the conductivity of the films increases as the optical band gap decreases. Moreover, the conductivity of the SnO_2 thin films increases with higher post annealing temperatures.

- **Data Avalability:** The data that are used in this research are available to the corresponding authors which will be providing upon request.
- **Funding:** The authors have not disclosed any funding
- **Ethical Declarations:** There have no conflict to declare.

REFERENCES

[1]. Wohlmuth W and Adesida I; Thin Solid Films; 479; 2005; 223.
[2]. Matsubara K, Fons P, Iwata K, Yamada A, Sakurai K, Tampo H and Niki S; Thin Solid Films; 431; 2003; 369.
[3]. Kikuchi N, Kusano E, Kishio E and Kingara A; Vacuum; 66; 2002; 365.
[4]. Man-Soo H, Lee H J, Jeong H S, Seo Y W and Kwon S J; Surf. Coat. Technol.; 29; 2003; 171.
[5]. Cao H, Qiu X, Liang Y, Zhang L, ZhaoMand Zhu Q; Chem. Phys. Chem.; 7; 2006; 497.
[6]. He H Jr, Wu T H, Hsin C L, Li K M, Chen L J, Chueh Y L, Chou L J and Wang Z L; Small; 2; 2006; 116.
[7]. Chaudhuri U R, Ramkumar K and Satyam M; J. Phys. D: Appl. Phys; 23; 1990; 994.
[8]. F. F. Liu, B. Shan, S. F. Zhang, and B. T. Tang, Langmuir 34(13); 2018; 3918–3924.
[9]. L. B. Xiong, Y. X. Guo, J. Wen, H. R. Liu, G. Yang, P. L. Qin, and G. J. Fang, Adv. Funct. Mater. 28(35); 2018; 1802757.
[10]. S. H.Wu, Y. T. Li, J. S. Luo, J. Lin, Y. Fan, Z. H. Gan, and X. Y. Liu, Opt. Express 22(4); 2014; 4731–4737.
[11]. H. Yu, H. I. Yeom, J. W. Lee, K. Lee, D. Hwang, J. Yun, J. Ryu, J. Lee, S. Bae, S. K. Kim, and J. Jang, Adv. Mater. 30(10); 2018; 1704825.
[12]. Q. Jiang, X. W. Zhang, and J. B. You, Small 14(31); 2018; 1801154.
[13]. S. Parveen Banu, T. Saravana Kumaran, S. Nirmala and J. Dhanakodi; American Journal of Engineering Research (AJER); 2; 2013; 131.
[14]. Noikaew, B., Chinvetkitvanich, P., Sripichal I. and Chityuttakan, C.; Journal of Metals; Materials and Minerals 18 (2); 2008; 49.
[15]. Chako S, Philip N S and Vaidyan V K; Phys. Stat. Sol. (a); 204; 2007; 3305.
[16]. Tewari S., and Bhattacharjee A., Pramana J. Phys.; 76; 2011; 153–163.
[17]. Kim K H and Chun J S; Thin Solid Films; 141; 1986; 287.
[18]. Islam M.J, Khatun N, Bhuiyan RH, Sultana S, Shaikh MA, Bitu MAB, Chowdhury F, Islam S RSC Adv.; 13; 2023; 19164.
[19]. C. V. Ramana, R. J. Smith, and O. M. Hussain; phys. stat. sol. (a); 199; 2003; R4–R6.
[20]. Soumia Belhamri, Nasr-Eddine Hamdadou; Journal of Physics: Conference Series 758; 2016; 12007.
[21]. Tauc, J., R. Grigorovici and A. Vancu; Physica Status Solidi; 15; 1966; 627-637.
[22]. Davis, E.A. and N.F. Mott; Philosophical Magazine; 22; 1970; 903.
[23]. Mott, N.F. and E.A. Davis; Electronic processes in non-crystalline materials; 2nd ed.; 1979; Clarendon Press (Oxford and New York).
[24]. Brian D. Viezbicke, Shane Patel, Benjamin E. Davis, and Dunbar P. Birnie; Physica Status Solidi; B, 252; 2015; 1700-1710.
[25]. A.A. Yadav E.U. Masumdara, A.V. Moholkarb, M. Neumann-Spallartc, K.Y. Rajpured, C.H. Bhosaled; Journal of Alloys and Compounds; 488; 2009; 350–355.
[26]. Saeideh Ebrahimiasl, Wan Md. Zin Wan Yunus, Anuar Kassim, and Zulkarnain Zainal MDPI; 11(10); 2011; 9207–9216.
[27]. Wiktor Matysiak, Tomasz Tański, Weronika Smok & Oleg Polishchuk; Scientific Reports; 10; 2020; 14802.
[28]. B. Sawickia, E. Tomaszewiczb, M. Piatkowskab, T. Grona, H. Dudaa and K. Górnya; ACTA PHYSICA POLONICA A; 129; 2016; 94.